Oral Oncology 91 (2019) 21–28

Contents lists available at ScienceDirect

Oral Oncology

journal homepage: www.elsevier.com/locate/oraloncology

Differences of tumor-recruiting myeloid cells in murine squamous cell carcinoma influence the efficacy of immunotherapy combined with a TLR7 agonist and PD-L1 blockade

Hidetake Tachinami[a,b], Naoto Nishii[a,c], Yulong Xia[a], Yoshihisa Kashima[a,c], Tatsukuni Ohno[a], Shigenori Nagai[a], Lixin Li[d], Walter Lau[d], Kei Tomihara[b], Makoto Noguchi[b], Miyuki Azuma[a,*]

[a] Department of Molecular Immunology, Graduate School of Medical and Dental Sciences, Tokyo Medical and Dental University, 1-5-45 Yushima, Bunkyo-ku, Tokyo 113-8549, Japan
[b] Department of Oral and Maxillofacial Surgery, Graduate School of Medicine and Pharmaceutical Sciences for Research, University of Toyama, 2630 Sugitani, Toyama City, Toyama 930-0194, Japan
[c] Department of Oral and Maxillofacial Surgery, Graduate School of Medical and Dental Sciences, Tokyo Medical and Dental University, 1-5-45 Yushima, Bunkyo-ku, Tokyo 113-8549, Japan
[d] Birdie Biopharmaceuticals Inc., Iselin, NJ 08830, USA

ARTICLE INFO

Keywords:
Myeloid-derived suppressor cells (MDSC)
TLR7 agonist
Immune checkpoint inhibitor
Squamous cell carcinoma (SCC)
Tumor-infiltrating lymphocytes (TIL)
Anti-tumor immunity
Immunotherapy
Murine model

ABSTRACT

Objectives: The immune status of the tumor microenvironment has a marked impact on clinical outcomes. Here we examined the immune environments of tumor-infiltrating leukocytes (TILes) in two murine models of squamous cell carcinoma and compared the effects of immunotherapeutic agents, including a TLR7 agonist and an immune checkpoint inhibitor, and a chemotherapeutic agent, gemcitabine, in these models.
Materials and methods: TILes from NR-S1- and SCCVII-grafted mice were analyzed by flow cytometry. NR-S1-inoculated mice received resiquimod (a synthetic TLR7 agonist), an anti-PD-L1 antibody, or both, and tumor growth and TILs were examined. Gemcitabine was administered to deplete $CD11b^+$ cells.
Results: More than 50% of TILes from NR-S1- and SCCVII-inoculated mice were $CD11b^+Gr\text{-}1^+$ cells. A major fraction of NR-S1 $CD11b^+$ cells was $Ly6G^{high}Ly6C^{low\text{-}nega}F4/80^-$ tumor-associated neutrophils (TANs) and the majority of SCCVII $CD11b^+$ cells were $Ly6G^{low}Ly6C^-F4/80^+$ tumor-associated macrophages. NR-S1 TANs did not express MHC class II and CD86, but did express reactive oxygen species and PD-L1. Resiquimod, alone and in combination with an anti-PD-L1 antibody, did not regress NR-S1 tumors, but the combination increased the CD8/regulatory T cell-ratio, and IFN-γ and PD-1 expression in $CD8^+$ TILes. Pre-administration of low-dose gemcitabine prior to the combination treatment suppressed the progression of NR-S1 tumors.
Conclusions: NR-S1 tumors with abundant recruitment of TANs were resistant to treatments with a TLR7 agonist, alone and in combination with PD-1 blockade, and required an additional gemcitabine treatment. The phenotype and status of tumor-infiltrating $CD11b^+$ myeloid cells may influence the efficacy of immunotherapeutic agents.

Introduction

Head and neck squamous cell carcinoma (HNSCC) is the sixth most common cancer globally and has a high mortality rate; moreover, a substantial proportion of patients suffer recurrent and metastatic disease [1,2]. Monotherapy with an immune-checkpoint inhibitor (ICI), such as nivolumab or pembrolizumab (anti-PD-1 antibody), provides considerable benefit but the overall response rate in patients with recurrent and metastatic HNSCC is less than 20% [3,4]. To improve the efficacy of ICI treatment, it is important to identify markers predictive of a response to therapy.

The immune status of the tumor microenvironment (TME) exerts a marked impact on clinical outcomes [5]. The reproducibility and prognostic power of $CD3^+$ and $CD8^+$ tumor-infiltrating lymphocyte (TIL) densities were validated in colon cancer [6]. TILs comprise various immunostimulatory and immunoregulatory cell types. The immune environment varies among tissues and by degree of tumor differentiation, as well as among individual patients. A recent tissue microarray analysis of HNSCC showed that infiltration of all types of T cells, including $CD8^+$, $CD4^+$, and regulatory T cells (Treg) is an

* Corresponding author.
E-mail address: miyuki.mim@tmd.ac.jp (M. Azuma).

https://doi.org/10.1016/j.oraloncology.2019.02.014
Received 9 November 2018; Received in revised form 7 February 2019; Accepted 14 February 2019
Available online 20 February 2019
1368-8375/

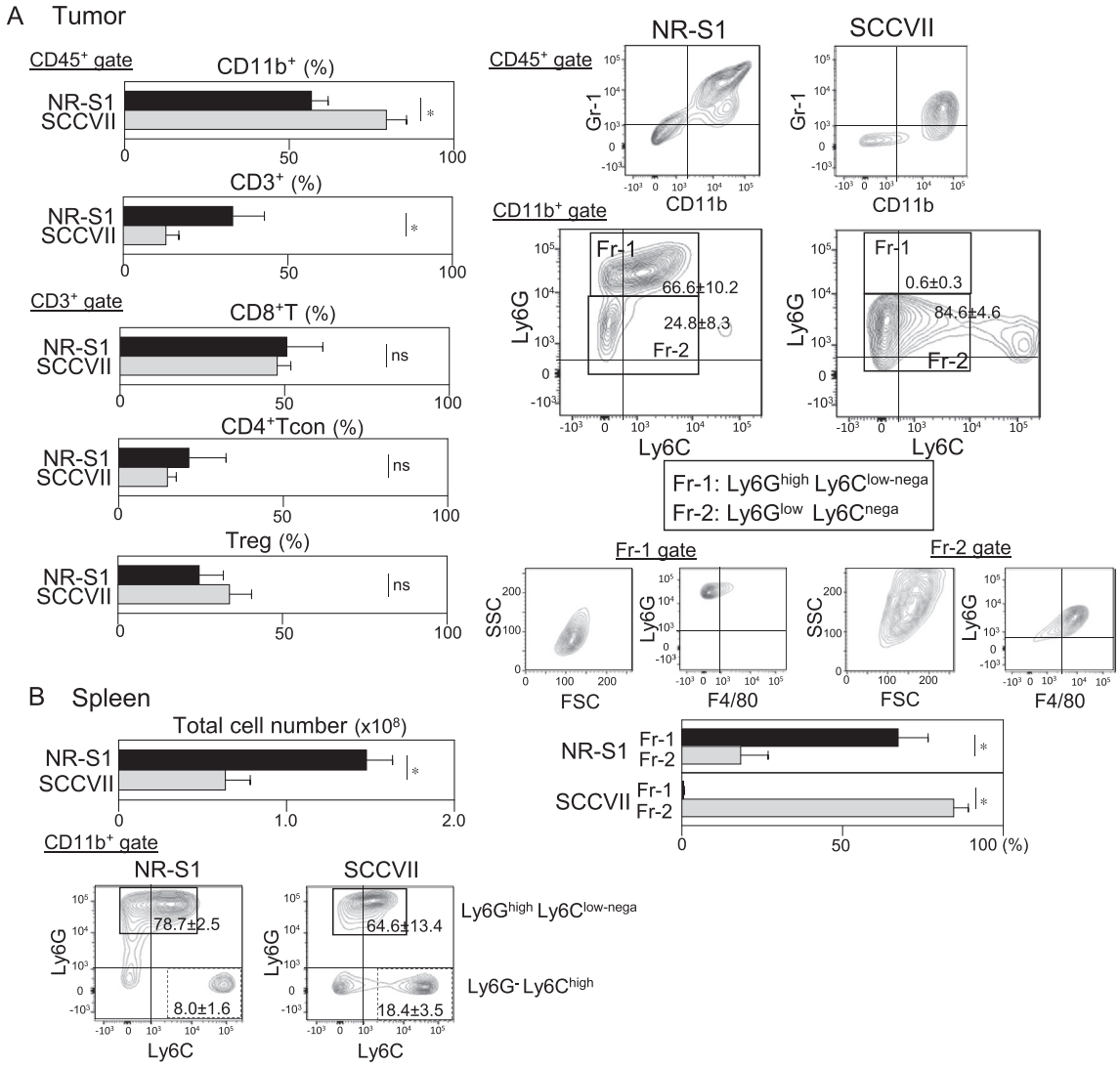

Fig. 1. NR-S1 and SCCVII tumors exhibit different CD11b$^+$ cell profile in the tumor microenvironment (TME). NR-S1 and SCCVII cells were inoculated, and the tumor masses and spleens were resected when the tumor volume reached around 1500 mm^3. (A) Tumor-infiltrating leukocyte (TILe)-fractions were stained with fluorochrome-conjugated anti-CD45, anti-CD3, anti-CD11b, and either anti-Gr-1, anti-Ly6C, anti-Ly6G, and anti-F4/80, or anti-CD4, anti-CD8, and Foxp3 mAbs and analyzed by flow cytometry. Electronic gates were placed on CD45$^+$FSC$^{low\text{-}high}$ large-lymphocytes (CD45$^+$ gate), FSC^{low}CD3$^+$CD11b$^-$ lymphocytes (CD3$^+$ T-gate), FSC$^{low\text{-}high}$CD3$^-$CD11b$^+$ myeloid cells (CD11b$^+$ gate), Ly6G^{high}Ly6C$^{low\text{-}nega}$ cells (Fr-1 gate), and Ly6G^{low}Ly6C$^{low\text{-}nega}$ cells (Fr-2 gate) and then the proportions and expression profiles (as contour plots) of the indicated populations are shown. For T-cell analysis, the proportions of CD8$^+$CD4$^-$ (CD8$^+$) T cells, CD8$^-$CD4$^+$Foxp3$^-$ T cells (conventional T cells, CD4$^+$ Tcon), and CD8$^-$CD4$^+$Foxp3$^+$ (regulatory T cells, Tregs) are shown. (B) Total splenocytes were counted and cells were stained with fluorochrome-conjugated anti-CD3, anti-CD11b, anti-Ly6C, and anti-Ly6G mAbs and analyzed by flow cytometry. An electronic gate was placed on CD3$^-$CD11b$^+$ cells (CD11b$^+$ gate), and the expression profiles of Ly6C and Ly6G were assessed; these are shown as contour plots. All quadrant markers were positioned to include > 95–98% of control fluorochrome-stained cells. Values are means ± SD (n = 5). $^*p < 0.05$.

independent prognostic factor [7], and suggested that so-called 'inflamed tumors' have a better prognosis. HNSCC frequently has an immunocompromised and TGF-β signaling-rich TME [8,9]. Therefore, in addition to T-cell-centered immune evaluation, factors unique to HNSCC also deserve attention.

We previously examined the effect of treatment with an anti-PD-L1 monoclonal antibody (mAb; PD-L1 blockade) in NR-S1 and SCCVII murine models of SCC, both of which originated from the C3H strain. NR-S1 is more sensitive to PD-L1 blockade, but the single treatment cannot eradicate either of the tumors [10,11]. We recently reported that systemic administration of low-dose resiquimod, a synthetic agonist of Toll-like receptor (TLR) 7, enhanced early activation of dendritic cells (DCs), resulting in enhanced priming of CD8$^+$ T cells and a decreased Treg frequency, which suppressed the growth of SCCVII tumors [11]. The combination of resiquimod and PD-L1 blockade markedly regressed the growth of SCCVII tumors. Thus, resiquimod has potential as an adjunct to PD-1/PD-L1 blockade therapy. The proportion of CD11b$^+$Gr-1$^+$ cells in TILs from both NR-S1 and SCCVII tumor-bearing mice increased with tumor progression, but the phenotypic profiles of these cells were different [12–15].

Gemcitabine (Gem) is a deoxycytidine analog antimetabolite with anti-tumor activity. Gem has been shown to selectively eliminate CD11b$^+$Gr-1$^+$ cells in several murine tumor models and reduce myeloid cells in patients with pancreatic cancer [14,16–18].

In this study, we performed a comparative analysis of tumor-infiltrating CD11b$^+$Gr-1$^+$ cells in two models of SCC and examined the efficacy of resiquimod and/or PD-L1 blockade, with or without gemcitabine pretreatment, against NR-S1 tumors.

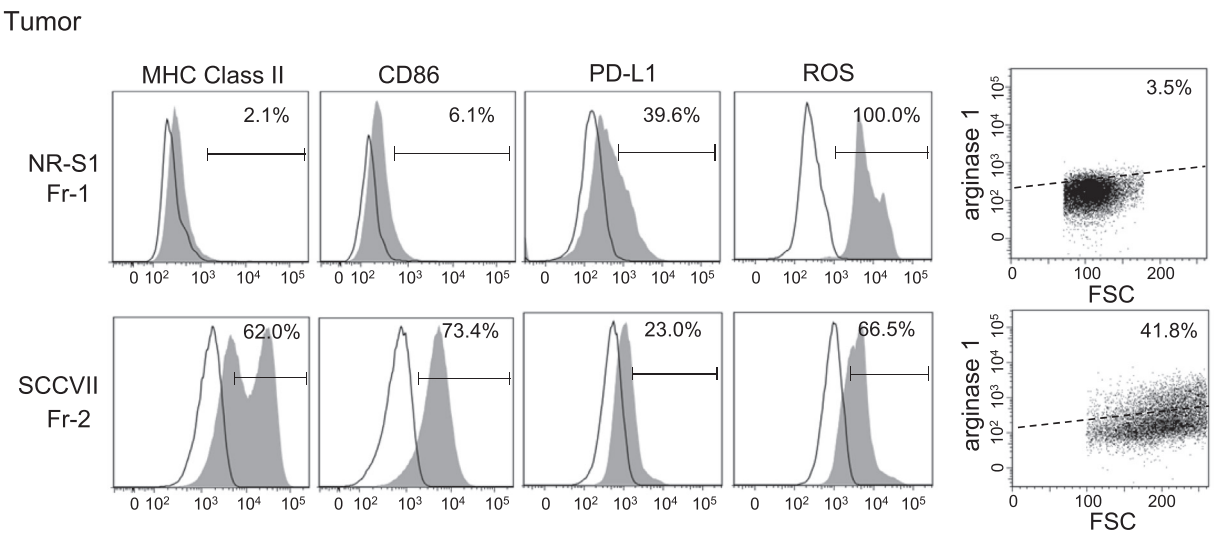

Fig. 2. Expression of functional molecules in NR-S1 Fr-1- and SCCVII Fr-2-TILes. TILes were obtained as described in Fig. 1A. Cell-surface expression of MHC class II, CD86, and PD-L1, and intracellular expression of arginase 1 and reactive oxygen species (ROS) were determined. Electronic gates were set for Fr-1 and Fr-2; the expression levels of the indicated factors are displayed as gray histograms with the controls as open histograms, or dotted plot with forward scatter (x-axis). Data are representative of three mice with similar results. Values in the right corners are positive percentages.

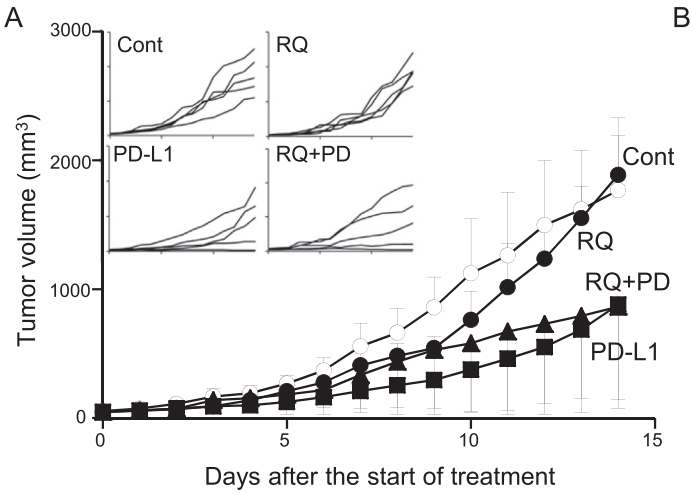

Fig. 3. Effect of resiquimod and/or PD-L1 blockade on NR-S1 tumor growth. NR-S1 cells were inoculated into C3H mice, and treatments were started at a tumor volume of 30 mm^3. Control reagents (PBS or rat IgG), resiquimod (RQ), anti-PD-L1 mAb (PD-L1) and both (RQ + PD) were injected intraperitoneally four times at 3-days intervals. Tumor volume was measured daily. (A) Values are means ± SD (n = 5). Left small panels, individual growth curves. (B) Tumor volumes at 14 days after the start of treatment are shown. Data are representative of two independent experiments with similar results.

Materials and methods

Mice

Female C3H/HeN (C3H) mice (6–7-weeks of age) were purchased from Japan SLC (Hamamatsu, Japan). All mice were maintained under specific pathogen-free conditions at Tokyo Medical and Dental University. All experimental procedures were reviewed and approved by the Animal Care and Use Committee of Tokyo Medical and Dental University (0170344A and A2018-262C).

Inoculation of SCC cells and treatment

NR-S1 [10,19] and SCC VII [20,21] are murine SCC cell lines of C3H origin. A subline of NR-S1 (NR-S1K) [12,15] was used in this study. The expression profiles of MHC class I and PD-L1, after stimulation with or without IFN-γ, are shown in Supplementary Fig. 1. Cultured SCC cells were freeze stocked simultaneously, and cells that had been cultured for 5–7 days were used for tumor inoculation. NR-S1 (1×10^6 cells) and SCCVII (2×10^5 cells) cells were injected subcutaneously (s.c.) into the shaved right flank of syngeneic C3H mice, and tumor volumes were estimated using the following equation: tumor volume (mm^3) = [long length (mm) × short length $(mm)^2$]/2 [22,23]. Treatment was started when the tumor volume of individual mice reached 30 mm^3 (6–8 days after tumor inoculation). Resiquimod (1.7 μg/mouse) and/or an anti-PD-L1 mAb (MIH5, rat IgG2a, 200 μg/mouse) [24] were intraperitoneally administrated four times at 3-day intervals [10,11,24]. For control group, PBS or rat IgG (Sigma-Aldrich) was administrated. In some experiments, gemcitabine (30 mg/kg, Wako, Osaka, Japan) was intraperitoneally injected 1 day before the initial treatment.

Isolation of tumor-infiltrating leukocytes (TILes)

TILes were isolated by digestion with collagenase I, hyaluronidase, and DNase and density-gradient centrifugation, as described previously [11].

Monoclonal antibodies and flow cytometry

Monoclonal antibodies (mAbs) against CD3 (17A2, rat IgG2b), CD4 (GK1.5, rat IgG2b), CD8 (53-6.72, rat IgG1), CD45 (30-F11, rat IgG2b), IFN-γ (XMG1.2, rat IgG1), Foxp3 (FJK-165, rat IgG2a), CD11b (M1/70, rat IgG2b), Gr-1 (Ly6C/Ly6G, RB6-8C5, rat IgG2b), Ly6C (HK1.4, rat IgG2c), Ly6G (1A8, rat IgG2a), F4/80 (BM8, rat IgG2a), CD86 (PO3.1, rat IgG2b), MHC class II (M5/114, rat IgG2b), PD-1 (J43, Armenian hamster IgG), and PD-L1 (MIH5, rat IgG2a) were used. All

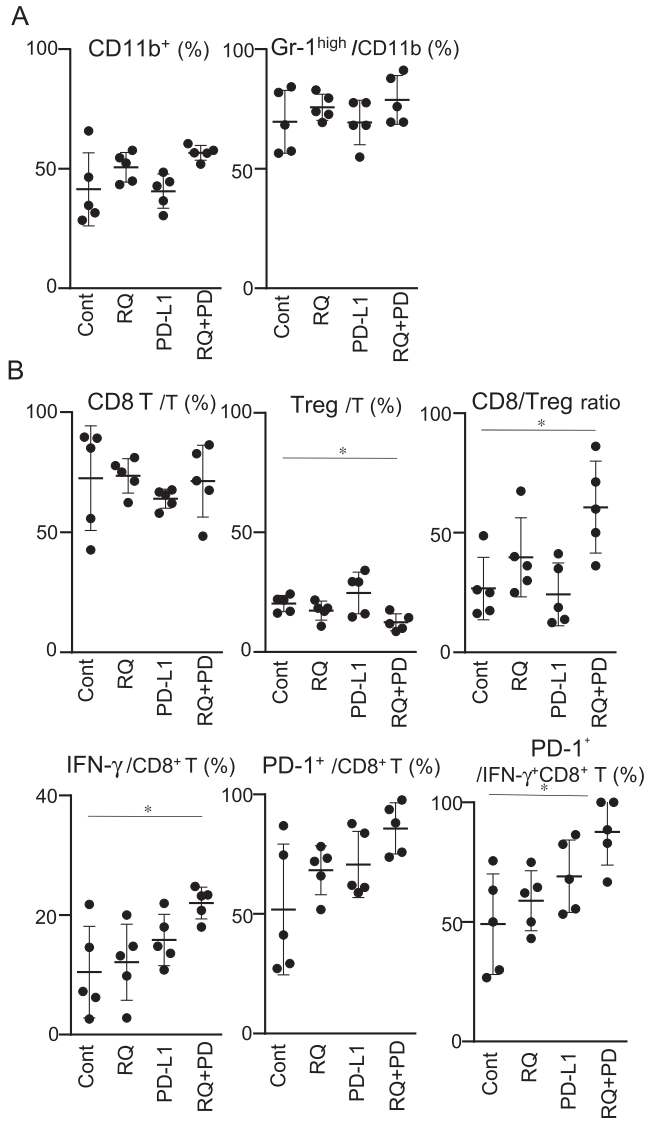

Fig. 4. Immunophenotypic changes of TILes. Tumor masses from NR-S1-inoculated mice were collected at 24 days after tumor inoculation and TILes were isolated. For analyses of $CD11b^+$ cells (A), the isolated cells were stained with anti-CD45, anti-CD3, anti-CD11b, and Gr-1 mAbs. For analysis of T cells (B), the cells were stimulated with phorbol-12 myristate-13-acetate (PMA), ionomycin, and brefeldin A for 6 h, and cells were stained with anti-CD45, anti-CD3, anti-CD4, anti-CD8, anti-Foxp3, anti-IFN-γ, and PD-1 mAbs or appropriate fluorochrome-conjugated control Abs. The stained cells were analyzed by flow cytometry. Electric gates were placed on large $CD45^+$ lymphocytes, $CD45^+CD3^+$ lymphocytes (T cells), $CD45^+CD3^+CD8^+$ ($CD8^+$ T cells), and $CD45^+CD3^+CD8^+IFN\text{-}\gamma^+$ cells, and their proportions were analyzed. Data are representative of two independent experiments with similar results. Bars show means ± SD (n = 5). $^*p < 0.05$.

fluorochrome (FITC, PE, PE-Cy7, PerCP-Cy5.5, APC, APC-eFluor780, eFluor450, and Brilliant Violet 510)-conjugated mAbs were obtained from Thermo Fisher Scientific (Carlsbad, CA), BD-Biosciences (San Jose, CA), or Biolegend (San Diego, CA). Blocking of non-specific binding via FcγR and multicolor cell staining for cell surface and intracellular (Foxp3, IFN-γ) molecules was performed as described previously [23]. For detection of reactive oxygen species (ROS), the CellRox® Green Flow Cytometry Assay Kit (Thermo Fisher Scientific) was used according to the manufacturer's protocol. For detection of arginase 1, cells were pre-stimulated with lipopolysaccharide (LPS) (100 ng/mL, Sigma-Aldrich L6511) for 4 h and subjected to multicolor cell surface and intracellular staining using a Foxp3 staining kit and PE-anti-arginase 1 antibody (R&D systems, Minneapolis, MN). Stained cells were analyzed using a FACSVerse flow cytometer (BD Biosciences) and a FlowJo software (Tree Star, Ashland, OR).

Statistical analysis

Statistical analyses were performed using the Mann–Whitney *U* test. A value of $p < 0.05$ was considered to indicate significance.

Results

Tumor-infiltrating $CD11b^+$ myeloid cell composition

We first analyzed the composition of $CD45^+$ TILes in 1500 mm^3 NR-S1 and SCCVII tumors grafted to syngeneic C3H mice. Interestingly, $CD11b^+$ cells constituted more than half of TILes in both tumors. The proportion of $CD11b^+$ cells in NR-S1 tumors was significantly lower than that in SCCVII tumors, and the proportion of $CD3^+$ T cells was higher (Fig. 1A). No clear difference in the proportions of the three major T-cell subsets ($CD8^+$ T cells, $Foxp3^-CD4^+$ conventional T cells (Tcon), and $Foxp3^+CD4^+$ Tregs) was observed between NR-S1 and SCCVII tumors. $CD11b^+$ cells showed different levels of Gr-1 expression (Fig. 1, upper right). Because the anti-Gr-1 antibody recognizes both Ly6C and Ly6G, we used specific a mAb specific for Ly6C or Ly6G. A major fraction of the $CD11b^+$ cells in NR-S1 tumors had a $Ly6G^{high}Ly6C^{low\text{-}nega}$ phenotype (Fr-1), whereas the majority of $CD11b^+$ cells in SCCVII tumors had a $Ly6G^{low}Ly6C^-$ phenotype (Fr-2). NR-S1 Fr-1 cells were forward scatter $(FSC)^{med}$, side scatter $(SSC)^{med}$, and $F4/80^-$, whereas SCCVII Fr-2 cells were FSC^{high}, SSC^{high}, and $F4/80^+$. The expression of F4/80 and Ly6G, cell size by FSC, and intracellular granule status by SSC indicated that Fr-1 and Fr-2 possess neutrophil- and macrophage-like phenotype, respectively [25,26]. NR-S1 $CD11b^+$ cells comprised ~60% Fr-1 and ~20% Fr-2 cells, whereas ~80% of SCCVII $CD11b^+$ cells were Fr-2.

Consistent with our previous report [12], spleens from NR-S1 tumor-bearing mice showed apparent splenomegaly and a twofold greater number of splenocytes than in SCCVII-bearing mice (Fig. 1B). Based on the expression profiles of Ly6C and Ly6G, $CD11b^+$ splenocytes were divided into three populations: $Ly6G^{high}Ly6C^{low}$, $Ly6G^-Ly6C^{high}$, and $Ly6G^{low/-}Ly6C^-$ cells. The former two populations present similar phenotype to polymorphonuclear-myeloid-derived suppressor cells (PMN-MDSCs) and monocytic-MDSCs (M-MDSCs), respectively [26]. The first population was similar phenotype to that of NR-S1 Fr-1 cells. The spleens of NR-S1 tumor-bearing mice contained a higher ratio of $Ly6G^{high}$ and lower ratio of $Ly6C^{high}$ cells.

Our results demonstrate that the immune status of the TMEs of the two SCC tumors are different, particularly in terms of $CD11b^+$ myeloid cells. $Ly6G^{high}$ $F4/80^-$ Fr-1 predominated in NR-S1 tumors, and $Ly6G^{low}$ $F4/80^+$ Fr-2 predominated in SCCVII tumors.

$Ly6G^{high}$ Fr-1 cells in NR-S1 express PD-L1 and ROS

We next examined functional molecule expression in Fr-1 and Fr-2 cells. MHC class II and CD86, critical cell-surface molecules required for antigen-presentation, were barely expressed on NR-S1 Fr-1, but were highly induced on SCCVII Fr-2 cells (Fig. 2). MHC class II expression in SCCVII Fr-2 cells had two peaks. Both Fr-1 and Fr-2 cells expressed the immune-checkpoint ligand PD-L1, but its expression was higher in NR-S1 Fr-1. ROS and arginase 1 (a cytosolic enzyme that downregulates nitric oxide production) are often correlated with immunosuppressive activity by MDSCs [27]. Most NR-S1 Fr-1 cells contained ROS but did not express arginase 1 to any significant degree. In contrast, a portion of SCCVII Fr-2 cells contained ROS and express arginase 1. Among NR-S1 TILes, Fr-2 cells had similar expression profiles of the above molecules to those of SCCVII Fr-2 cells (data not shown). Since phenotypic profile of NR-S1 Fr-1 cells was similar to that of PMN-MDSCs [26], we next

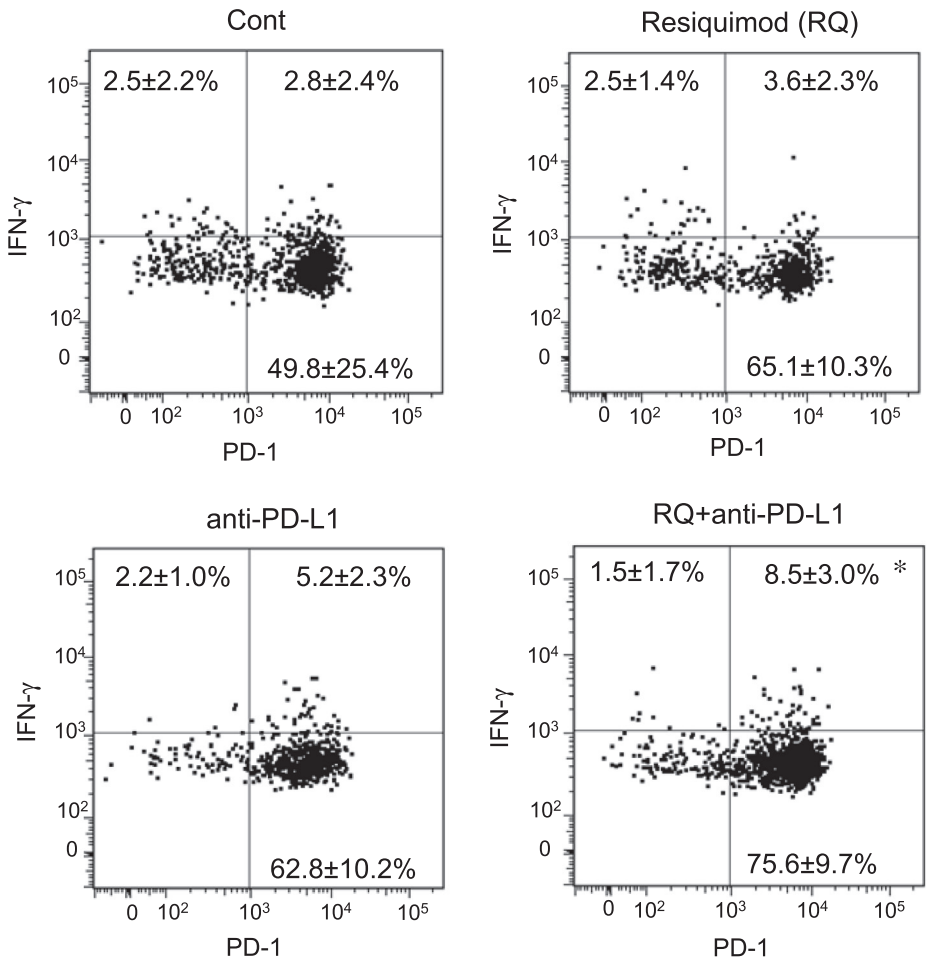

Fig. 5. Expression profiles of IFN-γ and PD-1 in $CD8^+$ TILs. TILes were isolated and stained as described in Fig. 4. An electric gate was placed on $CD45^+CD3^+CD8^+$ cells and the expression profiles of IFN-γ and PD-1 are shown as dotted plots. Quadrant markers were positioned to include > 97% of control fluorochrome-stained cells. Values are means ± SD (n = 5). *Significant difference from the control group ($p < 0.05$).

investigated inhibitory function of these cells in a T-cell suppression assay. The addition of $CD11b^+Gr\text{-}1^{high}$ cells isolated from the tumors and spleens of NR-S1 tumor-bearing mice did not suppress proliferative responses by $CD4^+$ and $CD8^+$ T cells stimulated with anti-CD3 and anti-CD28 mAbs (Supplementary Fig. 2). IFN-γ production by whole T cells was rather increased by the addition of $CD11b^+Gr\text{-}1^{high}$ cells.

NR-S1 Fr-1 expressed PD-L1 and contained ROS, but did not possess antigen-presenting ability and direct suppressive function to T cells. SCCVII Fr-2 contained both antigen-presenting immunostimulatory cells and immunoregulatory cells containing ROS and expressing arginase 1.

Resiquimod does not inhibit the growth of NR-S1 tumors

Low-dose systemic administration of resiquimod inhibited the growth of SCCVII tumors and, in combination with PD-L1 blockade, further reduced tumor growth by enhancing the CD8/Treg ratio of TILs [11]. In this study, resiquimod, which reduced the growth of SCCVII tumors, did not affect the growth of NR-S1 tumors (Fig. 3A and B). The anti-PD-L1 mAb treatment gradually decreased the mean tumor volume, but the final effects were individually variable. The combination of resiquimod and PD-L1 blockade did not exert any additional effect on tumor growth.

Combination treatment increases the CD8/Treg ratio and IFN-γ expression in TILs

We performed an immunophenotypic analysis of TILes on day 24. The proportions of $CD11b^+$ myeloid cells in TILes, and of $Gr\text{-}1^{high}$ Fr-1 in $CD11b^+$ cells, were not changed by any of the treatments (Fig. 4A). The combination of resiquimod and PD-L1 blockade decreased the percentage of Tregs, and increased the CD8/Treg ratio (Fig. 4B). The combination treatment increased the expression of the effector cytokine IFN-γ in $CD8^+$ TILs; however, the cell-surface expression of the immune-checkpoint receptor PD-1 was also increased (Figs. 4B and 5). The proportion of PD-1- and IFN-γ double-positive $CD8^+$ TILs was significantly increased by the combination treatment. Consistent with the $CD8^+$ TIL profiles, the combination treatment markedly increased the proportion of IFN-γ^+ cells in splenic $CD8^+$ T cells, which expressed PD-1 at a negligible level (data not shown). Therefore, none of the three treatments decreased the accumulation of Fr-1 cells in NR-S1 tumors, and all of them increased PD-1 expression on $CD8^+$ TILs.

Gemcitabine plus the combination treatment reduces NR-S1 tumor growth

The failure of NR-S1 tumor inhibition by the combination treatment may be due to persistent accumulation of $Ly6G^{high}$ Fr-1 cells. Multiple administrations of 60–120 mg/kg gemcitabine eliminated $Gr\text{-}1^+CD11b^+$ cells and enhanced antitumor immunity [14,16,17]. Therefore, we administered 30 mg/kg gemcitabine 1 day before the start of treatment. The percentage of $Gr\text{-}1^{high}CD11b^+$ peripheral blood

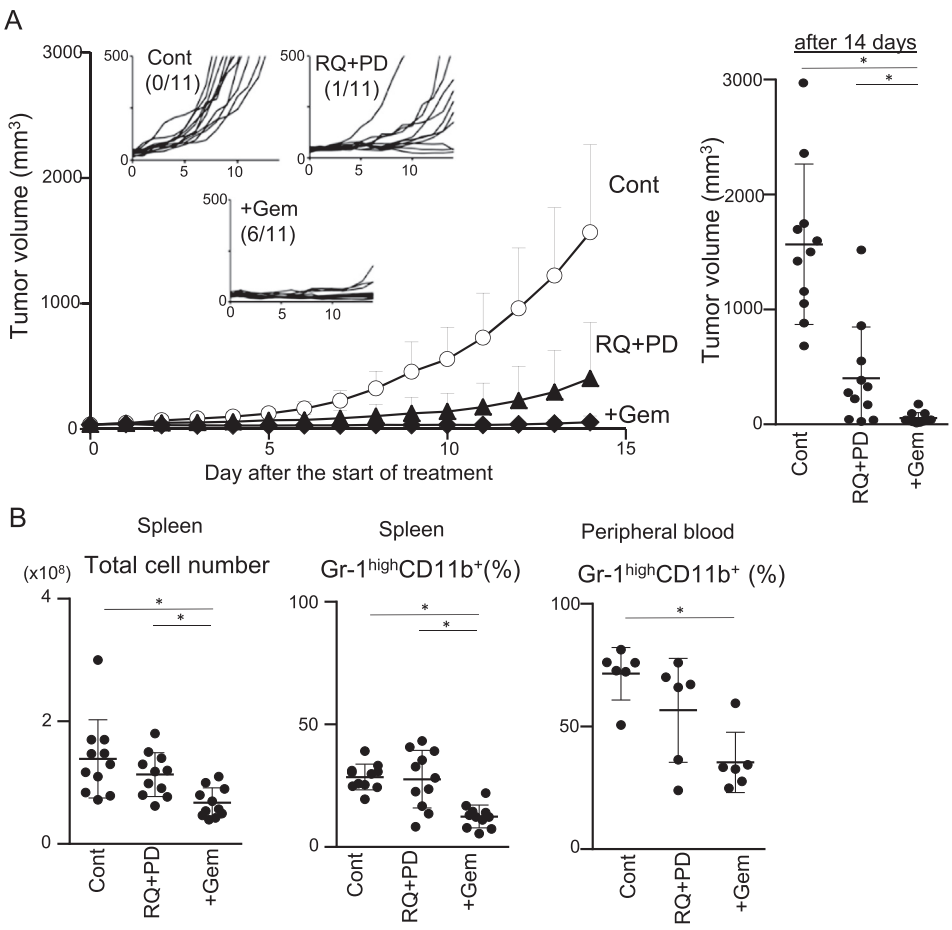

Fig. 6. Gemcitabine prior to the combination treatment prevents the growth of NR-S1 tumors. Inoculation of NR-S1 and treatments were conducted as described in Fig. 3. Gemcitabine (30 mg/kg) was intraperitoneally administered 1 day before the start of treatment with resiquimod and anti-PD-L1 mAb (+Gem). (A) Tumor volume was measured daily. Small panels at left, individual growth curves; values are the number of mice with a dormant tumor. Data are pooled from two independent experiments (n = 11). Right, tumor volumes at 14 days after the start of treatment. (B) Spleens were collected 24 days after tumor inoculation, and the total cell numbers were counted. Splenocyte and red blood cell-depleted peripheral blood leukocytes were stained with anti-CD11b and anti-Gr-1 mAbs and analyzed by flow cytometry. Percentages of Gr-1^{high}CD11b^+ cells are shown. Values for splenocytes are means ± SD (n = 11) of pooled two independent experiments. Values for peripheral blood are means ± SD (n = 6). $^*p < 0.05$.

cells was reduced by half 3 days after gemcitabine administration (data not shown). Addition of gemcitabine prevented the growth of NR-S1 tumors in most of the mice and significantly decreased the tumor volume at 14 days compared to the combination treatment (Fig. 6A). Six of eleven mice (54.5%) achieved a dormant tumor status. Because the tumors were too small to permit isolation of TILes, we analyzed spleens on the final experimental day. The addition of gemcitabine markedly reduced the total cell number and the proportion of Gr-1^{high}CD11b^+ cells as compared to those in the combination treatment group (Fig. 6B). The proportion of peripheral blood Gr-1^{high}CD11b^+ cells was also decreased by gemcitabine pretreatment. Low-dose gemcitabine, alone or together with resiquimod, did not reduce the volume of NR-S1 tumors (Supplementary Fig. 3). Our results demonstrate that elimination of Gr-1^{high}CD11b^+ cells at an earlier time point dramatically enhanced the efficacy of the combination of resiquimod and PD-L1 blockade against NR-S1 tumors.

Discussion

We here demonstrate that CD11b^+Gr-1^+ cells comprised over half of the TILs from two SCC tumors (NR-S1 and SCCVII), but their phenotypic profiles were different, and these differences greatly influence the efficacy of immunotherapy.

Phenotypic analysis of TILes at the late time point (Fig. 1) showed that tumor-infiltrating CD11b^+Gr-1^+ cells comprised Fr-1, Ly6-G^{high}Ly6C^-F4/$80^-$$FSC^{low}$$SSC^{med}$ and Fr-2, Ly6G^{low}y6$C^{low\text{-}nega}$F4/$80^+$$FSC^{high}$$SSC^{high}$ cells. The Fr-1 cells showed: (i) high expression of granulocyte marker Ly6G, (ii) lack of expression of the monocyte/macrophages markers Ly6C and F4/80, (iii) minimal expression of antigen presentation-related molecules, MHC class II and CD86, (iv) marginal arginase 1 expression, and (v) no suppressive function to T cells *ex vivo*. These results indicate that Fr-1 cells are prefer to be called tumor-associated neutrophils (TANs) rather than PMN-MDSCs. The Fr-2 cells showed (i) low Ly6G and lack of Ly6C expression, (ii) high F4/80 expression, and (iii) a large cell size and intracellular granules. These results indicate that Fr-2 cells are tumor-associated macrophages (TAMs), but not M-MDSCs because of lack of Ly6C expression. Although Ly6G^-Ly6C^+ M-MDSC-like cells were observed in spleens from both tumor-bearing mice, they were a minor fraction of the TILs at the late time point. The proportions of Ly6G^-Ly6C^+ cells in TILes were higher at earlier time points, and in mice with smaller tumors (data not shown). This indicates that tumor-recruiting Ly6C^+ monocytic cells are converted to Ly6C^-F4/80^+ TAMs during tumor progression, in agreement with a previous report [26]. The differential expression profiles of MHC class II, ROS, and arginase 1 in SCCVII Fr-2 cells suggest that TAMs include immunostimulatory (anti-tumor) and immunoregulatory (tumor-promoting) macrophages. Further studies are required to determine the function of SCCVII-associated TAMs.

Resiquimod did not exhibit efficacy against NR-S1 tumors, unlike against SCCVII [11]. In addition, despite the marked elevation of the CD8/Treg ratio (which is closely correlated with the tumor growth), and of the ratio of IFN-γ-expressing $CD8^+$ TILs (functional cytotoxic T lymphocytes), the combination treatment did not inhibit the tumor growth of NR-S1. This may be due to accumulation of TANs and the elevation of PD-1 expression on $CD8^+$ TILs. Although resiquimod treatment markedly decreased the accumulation of TAMs in SCCVII [11], none of resiquimod, PD-L1 blockade, or both suppressed the accumulation of TANs, which expressed PD-L1 (Fig. 3 and [15]). The combination treatment increased the number of IFN-γ-expressing activated $CD8^+$ TILs, but concurrently upregulated PD-1 expression. The most critical effect of resiquimod is activation of DCs [11]. It is possible that, in NR-S1 tumors, accumulating TANs may physically disrupt the

interactions of activated DCs with T cells in the TME, and may also induce PD-L1-mediated co-inhibitory signaling to the PD-1-expressing tumor-infiltrating T cells by trans-coinhibition as we described previously [28]. The high level of ROS in NR-S1 TANs may modulate the immunoregulatory TME. Thus, the priming and effector functions of $CD8^+$ T cells might be suppressed in the presence of Gr-$1^{high}CD11b^+$ cells in both lymphoid and tumor tissues. Earlier depletion of Gr-$1^{high}CD11b^+$ cells by low-dose gemcitabine may restore normal cell-cell interactions and induce a switch from an immunoregulatory to an immunostimulatory TME. Similar to the M1- and M2-like phenotypes of TAMs [25], TANs also exhibit N1 (anti-tumor)- and N2 (tumor-promoting)-like features [29]. The unique TME in NR-S1 tumors may polarize towards an N2-dominant status. Further studies are required to clarify suppressive mechanisms of TANs in the TME.

In human, peripheral blood samples have been used for most analyses of $CD11b^+$ myeloid cells in tumor-bearing patients and functional activity has not been confirmed. Therefore, it is difficult to discriminate general circulating neutrophils and PMN-MDSCs in human. The peripheral blood PMN-MDSCs defined as $CD11b^+HLA\text{-}DR^-CD14^-CD33^+$ cells are associated with progression of HNSCC [30]. A high neutrophil-to-lymphocyte (NLR) ratio in peripheral blood has a strong correlation with the number of circulating PMN-MDSCs (defined as $CD11b^+HLA\text{-}DR^-CD14^-CD15^+$) and a poor prognosis in HNSCC [31]. A standard gemcitabine chemotherapy in patients with pancreatic cancer showing a characteristic immunosuppressive TME transiently reduced peripheral blood PMN-MDSCs with elevation of $CD8^+$ T/Treg ratio [18]. Gemcitabine shows potential for combined chemotherapy and chemoradiotherapy in patients with HNSCC [32,33]. Thus, in patients with high numbers of circulating PMN-MDSCs (or a high NLR), use of gemcitabine may increase the efficacy of ICIs and TLR7 agonists. Comparative analyses of tumor-infiltrating and circulating myeloid cells in human samples, and identification of suitable markers to discriminate neutrophils and PMN-MDSCs are needed.

In summary, we distinguished between tumor-associated neutrophils and macrophages in two murine SCC graft models and demonstrated that the differences of $CD11b^+$ myeloid cell composition influence the immunotherapeutic efficacy of a TLR7 agonist, alone and in combination with PD-L1 blockade. Assessment of the phenotypic features of $CD11b^+$ myeloid cells in HNSCC might enable prediction of the efficacy of ICIs, both alone and in combination with agents of other classes.

Acknowledgements

This work was supported by the Japan Society for the Promotion of Science (JSPS) Grants-in-Aid for Scientific Research (KAKENHI) (A26253086, A18H04066 to M.A.).

Conflict of interest statement

Lixin Li and Walter Lau are employees of Birdie Biopharmaceuticals Inc. Other authors declare no competing financial interests.

Appendix A. Supplementary material

Supplementary data to this article can be found online at https://doi.org/10.1016/j.oraloncology.2019.02.014.

References

[1] Moy JD, Moskovitz JM, Ferris RL. Biological mechanisms of immune escape and implications for immunotherapy in head and neck squamous cell carcinoma. Eur J Cancer 2017;76:152–66.
[2] Lala M, Chirovsky D, Cheng JD, Mayawala K. Clinical outcomes with therapies for previously treated recurrent/metastatic head-and-neck squamous cell carcinoma (R/M HNSCC): a systematic literature review. Oral Oncol 2018;84:108–20.
[3] Ferris RL, Blumenschein Jr G, Fayette J, Guigay J, Colevas AD, Licitra L, et al. Nivolumab vs investigator's choice in recurrent or metastatic squamous cell carcinoma of the head and neck: 2-year long-term survival update of CheckMate 141 with analyses by tumor PD-L1 expression. Oral Oncol 2018;81:45–51.
[4] Mehra R, Seiwert TY, Gupta S, Weiss J, Gluck I, Eder JP, et al. Efficacy and safety of pembrolizumab in recurrent/metastatic head and neck squamous cell carcinoma: pooled analyses after long-term follow-up in KEYNOTE-012. Br J Cancer 2018;119:153–9.
[5] Fridman WH, Pages F, Sautes-Fridman C, Galon J. The immune contexture in human tumours: impact on clinical outcome. Nat Rev Cancer 2012;12:298–306.
[6] Pages F, Mlecnik B, Marliot F, Bindea G, Ou FS, Bifulco C, et al. International validation of the consensus Immunoscore for the classification of colon cancer: a prognostic and accuracy study. Lancet 2018;391:2128–39.
[7] Nguyen N, Bellile E, Thomas D, McHugh J, Rozek L, Virani S, et al. Tumor infiltrating lymphocytes and survival in patients with head and neck squamous cell carcinoma. Head Neck 2016;38:1074–84.
[8] Moskovitz J, Moy J, Ferris RL. Immunotherapy for head and neck squamous cell carcinoma. Curr Oncol Rep 2018;20:22.
[9] Pang X, Tang YL, Liang XH. Transforming growth factor-beta signaling in head and neck squamous cell carcinoma: insights into cellular responses. Oncol Lett 2018;16:4799–806.
[10] Tsushima F, Tanaka K, Otsuki N, Youngnak P, Iwai H, Omura K, et al. Predominant expression of B7–H1 and its immunoregulatory roles in oral squamous cell carcinoma. Oral Oncol 2006;42:268–74.
[11] Nishii N, Tachinami H, Kondo Y, Xia Y, Kashima Y, Ohno T, et al. Systemic administration of a TLR7 agonist attenuates regulatory T cells by dendritic cell modification and overcomes resistance to PD-L1 blockade therapy. Oncotarget 2018;9:13301–12.
[12] Tanaka K, Jinhua P, Omura K, Azuma M. Multipotency of CD11bhighGr-1 + immature myeloid cells accumulating in oral squamous cell carcinoma-bearing mice. Oral Oncol 2007;43:586–92.
[13] Sunthamala N, Pientong C, Ohno T, Zhang C, Bhingare A, Kondo Y, et al. HPV16 E2 protein promotes innate immunity by modulating immunosuppressive status. Biochem Biophys Res Commun 2014;446:977–82.
[14] Tomihara K, Fuse H, Heshiki W, Takei R, Zhang B, Arai N, et al. Gemcitabine chemotherapy induces phenotypic alterations of tumor cells that facilitate anti-tumor T cell responses in a mouse model of oral cancer. Oral Oncol 2014;50:457–67.
[15] Fuse H, Tomihara K, Heshiki W, Yamazaki M, Akyu-Takei R, Tachinami H, et al. Enhanced expression of PD-L1 in oral squamous cell carcinoma-derived CD11b (+)Gr-1(+) cells and its contribution to immunosuppressive activity. Oral Oncol 2016;59:20–9.
[16] Suzuki E, Kapoor V, Jassar AS, Kaiser LR, Albelda SM. Gemcitabine selectively eliminates splenic Gr-1+/CD11b+ myeloid suppressor cells in tumor-bearing animals and enhances antitumor immune activity. Clin Cancer Res: Off J Am Assoc Cancer Res 2005;11:6713–21.
[17] Le HK, Graham L, Cha E, Morales JK, Manjili MH, Bear HD. Gemcitabine directly inhibits myeloid derived suppressor cells in BALB/c mice bearing 4T1 mammary carcinoma and augments expansion of T cells from tumor-bearing mice. Int Immunopharmacol 2009;9:900–9.
[18] Eriksson E, Wenthe J, Irenaeus S, Loskog A, Ullenhag G. Gemcitabine reduces MDSCs, tregs and TGFbeta-1 while restoring the teff/treg ratio in patients with pancreatic cancer. J Transl Med 2016;14:282.
[19] Mogi S, Sakurai J, Kohsaka T, Enomoto S, Yagita H, Okumura K, et al. Tumour rejection by gene transfer of 4–1BB ligand into a CD80(+) murine squamous cell carcinoma and the requirements of co-stimulatory molecules on tumour and host cells. Immunology 2000;101:541–7.
[20] O'Malley BW, Cope KA, Chen SH, Li D, Schwarta MR, Woo SL. Combination gene therapy for oral cancer in a murine model. Cancer Res 1996;56:1737–41.
[21] Khurana D, Martin EA, Kasperbauer JL, O'Malley Jr BW, Salomao DR, Chen L, et al. Characterization of a spontaneously arising murine squamous cell carcinoma (SCC VII) as a prerequisite for head and neck cancer immunotherapy. Head Neck 2001;23:899–906.
[22] Piao J, Kamimura Y, Iwai H, Cao Y, Kikuchi K, Hashiguchi M, et al. Enhancement of T-cell-mediated anti-tumour immunity via the ectopically expressed glucocorticoid-induced tumour necrosis factor receptor-related receptor ligand (GITRL) on tumours. Immunology 2009;127:489–99.
[23] Kondo Y, Ohno T, Nishii N, Harada K, Yagita H, Azuma M. Differential contribution of three immune checkpoint (VISTA, CTLA-4, PD-1) pathways to antitumor responses against squamous cell carcinoma. Oral Oncol 2016;57:54–60.
[24] Tsushima F, Iwai H, Otsuki N, Abe M, Hirose S, Yamazaki T, et al. Preferential contribution of B7–H1 to programmed death-1-mediated regulation of hapten-specific allergic inflammatory responses. Eur J Immunol 2003;33:2773–82.
[25] Noy R, Pollard JW. Tumor-associated macrophages: from mechanisms to therapy. Immunity 2014;41:49–61.
[26] Bronte V, Brandau S, Chen SH, Colombo MP, Frey AB, Greten TF, et al. Recommendations for myeloid-derived suppressor cell nomenclature and characterization standards. Nat Commun 2016;7:12150.
[27] Gabrilovich DI. Myeloid-derived suppressor cells. Cancer Immunol Res 2017;5:3–8.
[28] Kang S, Zhang C, Ohno T, Azuma M. Unique B7–H1 expression on masticatory mucosae in the oral cavity and trans-coinhibition by B7-H1-expressing keratinocytes regulating CD4(+) T cell-mediated mucosal tissue inflammation. Mucosal Immunol 2017;10:650–60.
[29] Fridlender ZG, Sun J, Kim S, Kapoor V, Cheng G, Ling L, et al. Polarization of tumor-associated neutrophil phenotype by TGF-beta: "N1" versus "N2" TAN. Cancer Cell 2009;16:183–94.
[30] Chen WC, Lai CH, Chuang HC, Lin PY, Chen MF. Inflammation-induced myeloid-

derived suppressor cells associated with squamous cell carcinoma of the head and neck. Head Neck 2017;39:347–55.
[31] Chen MF, Chen PT, Kuan FC, Chen WC. The predictive value of pretreatment neutrophil-to-lymphocyte ratio in esophageal squamous cell carcinoma. Ann Surg Oncol 2018.
[32] El Deen DA, Toson EA, El Morsy SM. Gemcitabine-based induction chemotherapy and concurrent with radiation in advanced head and neck cancer. Med Oncol 2012;29:3367–73.
[33] Maseki S, Ijichi K, Nakanishi H, Hasegawa Y, Ogawa T, Murakami S. Efficacy of gemcitabine and cetuximab combination treatment in head and neck squamous cell carcinoma. Mol Clin Oncol 2013;1:918–24.